Polyhedron 28 (2009) 621–629

Contents lists available at ScienceDirect

Polyhedron

journal homepage: www.elsevier.com/locate/poly

New organometallic Ru(II) and Fe(II) complexes with tetrathia-[7]-helicene derivative ligands

Maria Helena Garcia [a,*], Pedro Florindo [a], Maria de Fátima M. Piedade [b], Stefano Maiorana [c], Emanuela Licandro [c]

[a] Centro de Ciências Moleculares e Materiais, Faculdade de Ciências da Universidade de Lisboa, Ed.C8, Campo Grande, 1749-016 Lisboa, Portugal
[b] Centro de Química Estrutural, Instituto Superior Técnico, Universidade Técnica de Lisboa, Av. Rovisco Pais, 1049-001 Lisboa, Portugal
[c] Dipartimento di Chimica Organica e Industriale, Università degli Studi di Milano, Via C. Golgi, 19, I-20133 Milano, Italy

ARTICLE INFO

Article history:
Received 9 July 2008
Accepted 2 December 2008

Keywords:
Heterohelicenes
Tetrathia-[7]-helicene
Ruthenium(II)
Iron(II)
Monocyclopentadienyl

ABSTRACT

A series of organometallic complexes possessing new tetrathia-[7]-helicene nitrile derivative ligands [**TH-7**] as chromophores, of general formula [MCp(P–P)(NC{TH-[7]-Y}Z)][PF_6] (M = Ru, Fe, P–P = DPPE, Y = H, NO_2, Z = H, C≡N; M = Ru, L–L = $2PPh_3$, Y = H, Z = H) has been synthesized and fully characterized. ^{1}H NMR, FT-IR and UV–Vis. spectroscopic data were analyzed with in order to evaluate the existence of electronic delocalization from the metal centre to the coordinated ligand to have some insight on the potentialities of these new compounds as non-linear optical molecular materials. Slow crystallization of compound [$RuCp(PPh_3)_2$(NC{TH-[7]-H}H)][PF_6] **2Ru** revealed an interesting isomerization of the helical ligand with formation of two carbon-carbon bonds between the two terminal thiophenes, leading to the total closure of the helix (**2**∗**Ru**).

1. Introduction

The search for new organic and organometallic materials with significant non-linear optical (NLO) properties has been an area of considerable interest due to their relevance to optical device technology [1–6]. Nevertheless, the observation of even-order non-linearity is limited to the asymmetric crystallization of the bulk materials. Thus, chiral structures appear as ideal systems to investigate second-order NLO effects due to their intrinsic non-centrosymmetry, which allows these effects to be observed even in symmetric media such as chiral isotropic liquids [7]. Large chiral effects have been demonstrated in surface NLO responses of films of chiral molecules adsorbed at the air/water interface [8] and of Langmuir–Blodgett films of chiral polymers [9].

In this context, the intrinsically chiral structures of helicenes [10] make these compounds very attractive to be investigated, leading to several theoretical and experimental studies of carbohelicenes [11] and heterohelicenes [12]. The easier functionalization of thiaheterohelicenes, compared to carbohelicenes, allows the introduction of several different functional groups, either in the terminal thiophene rings (formyl, alkoxycarbonyl, trifluoromethyl, amide, trialkylsilyl, cyanoacrylic and acrylates) or in the central benzene rings (alkyl and electron-withdrawing groups such as alkoxycarbonyl and trifluoromethyl) [13]. The reported optimized synthesis of tetrathia-[7]-helicene (TH[7]) and the convenient preparation of the formyl derivative 2-CHO-TH[7] [13a] paved the way for the synthesis of a variety of substituted heterohelicenes.

The present work reports the synthesis of three new TH[7] derivatives, through the functionalization of one terminal thiophene ring with a nitrile group (**L1**), two terminal thiophene rings with two nitrile groups (**L2**) and one terminal thiophene group with one nitrile group followed by nitration in the benzene rings (**L3**). These new TH[7] derivatives were used as ligands for the synthesis of a new family of η^5-monocyclopentadienyl ruthenium(II) and iron(II) organometallic complexes represented by the general formulation [MCp(PP)(NC{TH-[7]-Y} Z)] [PF_6] (M = Ru(II), Fe(II), P–P = DPPE, Y = H, NO_2, Z = H, C≡N; M = Ru(II), L–L = $2PPh_3$, Y = H, Z = H).

The new compounds have been characterized by the usual FT-IR, UV–Vis, ^{1}H and ^{31}P NMR spectroscopic techniques. Nevertheless, the poor solubility of the compounds in common deuterated solvents did not allow the characterization by ^{13}C NMR. The crystallization of compound [$RuCp(PPh_3)_2$(NC{TH-[7]-H}H)] [PF_6] **2Ru**, by slow diffusion of *n*-hexane into an acetone solution of the compound, afforded single crystals suitable for X-ray diffraction studies. This revealed isomerization of the helical ligand, due to the formation of two new carbon–carbon bonds between the terminal thiophene rings, giving the new complex **2**∗**Ru**.

* Corresponding author. Tel.: +351 21 750 00 75/6; fax: +351 21 750 00 88.
E-mail address: lena.garcia@fc.ul.pt (M.H. Garcia).

0277-5387/$ - see front matter © 2008 Elsevier Ltd. All rights reserved.
doi:10.1016/j.poly.2008.12.036

2. Results and discussion

2.1. Synthesis of the tetrathia-[7]-helicene ligands *L1*, *L2* and *L3*

The synthesis of the TH[7] derived nitrile ligands, tetrathia-[7]-helicene-2-carbonitrile (**L1**), tetrathia-[7]-helicene-2,13-dicarbonitrile (**L2**) and tetrathia-[7]-helicene-2-carbonitrile (**L3**), bearing the nitro group in an unidentified position of the helix, is summarized in Scheme 1.

Tetrathia-[7]-helicene-2-carbaldehyde (**2**) was synthesized in good yield by electrophilic formylation of the α-anion of tetrathia-[7]-helicene, generated with *n*-BuLi at −78 °C in DMF, following Ref. [13a]. The ligand tetrathia-[7]-helicene-2-carbonitrile (**L1**) was synthesized from compound **2** and hydroxyl ammonium chloride in pyridine, with *in situ* dehydration by acetic anhydride.

The reaction of **L1** with nitric acid in acetic anhydride was carried out with the purpose of synthesizing tetrathia-[7]-helicene-13-nitro-2-carbonitrile, nitrated at the opposite end of the helix relatively to the nitrile group, as would be expected following our previous experience with benzo[1,2-b;4,3-b′]dithiophene derivative complexes [14]. However the analysis of the ^{1}H NMR spectrum of the obtained compound showed the presence of two doublets at 6.65 and 7.57 ppm (J_{HH} = 5.6 Hz), attributed to the thiophene ring protons, revealing that the nitration had occurred in one of the benzene rings. Nevertheless, substitution of the H on the two terminal thiophene rings was possible with two nitrile groups (**L2**), whilst the introduction of NO_2 in position 13 through an electrophilic substitution failed, thus demonstrating that the only way to functionalize the helical system in a regioselective manner is through the generation of anions in the positions 2 and 13 and the reaction with electrophilic reagents. ^{13}C NMR studies were not carried out due to the low solubility of the organic ligands in common deuterated solvents (acetone-d_6, chloroform-*d*, acetonitrile-d_3 and DMSO-d_6) even at high temperatures and, consequently, further characterization by *HMQC* and *HMBC* NMR techniques could not be applied to identify the position of the NO_2 group; therefore, the structure proposed for **L3** in Scheme 1 is simply one out of six possible structures.

Tetrathia-[7]-helicene-2,13-dicarbonitrile (**L2**) was synthesized by the reaction of tetrathia-[7]-helicene (**1**) with two equivalents of *n*-BuLi at −78 °C in DMF, affording tetrathia-[7]-helicene-2,13-dicarbaldehyde (**3**), which was used, without purification, in the reaction with hydroxylammonium chloride in pyridine, and dehydration *in situ* with acetic anhydride.

2.2. Synthesis of complexes [M(η^5-C$_5$H$_5$)(PP)(L)][PF$_6$]

Complexes of the general formula [M(η^5-C$_5$H$_5$)(PP)(L)][PF$_6$] (M = Ru and Fe, PP = DPPE, L = **L1**, **L2** and **L3**; M = Ru(II), (PP) = 2PPh$_3$, L = **L1**) were prepared by halide abstraction with TlPF$_6$ from the parent neutral complexes [M(η^5-C$_5$H$_5$)(PP)X] (M = Fe, X = I; M = Ru, X = Cl) in dichloromethane, in the presence of an adequate excess of the corresponding nitrile (Scheme 2).

The reactions were carried out at reflux, stirring overnight under inert atmosphere. The compounds were recrystallized by slow diffusion of n-hexane in acetone or dichloromethane, affording microcrystalline products with colours ranging from orange to dark red. The compounds were fairly stable in air and moisture, both in the solid state and in solution, and were obtained in fair yields of 27–56%. The formulation of the new compounds is supported by analytical data, FT-IR and ^{1}H, ^{31}P NMR spectroscopic data, with the exception of compounds **L3** and **2Ru**, for which the elemental analysis always gave a significant error. Nevertheless, the elemental percentages for **L3** containing complexes are in good agreement with the proposed formulations. An effort is currently being made at our laboratory to obtain suitable crystals for X-ray diffraction studies of any of the compounds **L3**, **4Ru** and **4Fe**, so that the structure of **L3** can be unequivocally determined.

The solid state FT-IR spectra (KBr pellets) of the complexes presented the characteristic bands of the cyclopentadienyl ligand (≈ 3060 cm^{-1}), the PF_6^- anion (840 and 560 cm^{-1}) and the coordinated nitrile (ν_{CN} from 2214 to 2191 cm^{-1}) in all of the studied complexes. As observed for other ruthenium and iron related compounds,[14,15] negative shifts were found for ν_{CN}, compared to the corresponding values of the uncoordinated nitrile, in particular for the iron compound containing the coordinated TH-[7] functionalized with the strong acceptor NO_2 group (**L3**), where a shift of −24 cm^{-1} was found. Negative shifts in the nitrile and acetylide

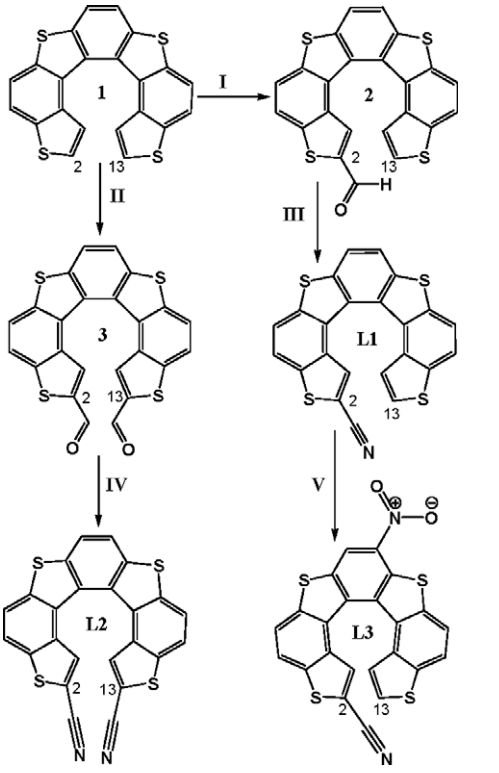

Scheme 1. Synthesis of ligands **L1**, **L2** and **L3**. **I** –THF, −78 °C, (i) *n*-BuLi, (ii) DMF [13a]; **II** – THF, −78 °C, (i) *n*-BuLi, (ii) DMF; **III** – (i) $HONH_2 \cdot HCl$, (ii) Ac_2O; **IV** – (i) $HONH_2 \cdot HCl$, (ii) Ac_2O; **V** – HNO_3/Ac_2O.

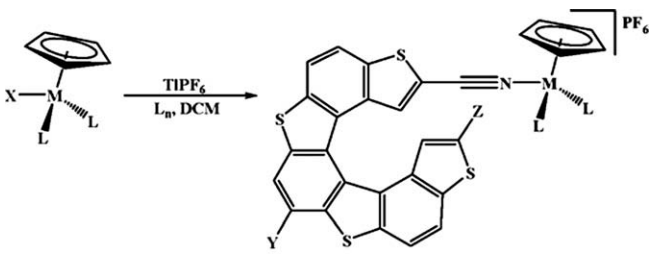

1Ru	M=Ru; (LL) = DPPE; L1 (Z=H ; Y=H)
1Fe	M=Fe; (LL) = DPPE; L1 (Z=H ; Y=H)
2Ru	M=Ru; (LL) = 2PPh$_3$; L1 (Z=H ; Y=H)
3Ru	M=Ru; (LL) =DPPE; L2 (Z=C≡N; Y=H)
3Fe	M=Fe; (LL) = DPPE; L2 (Z=C≡N; Y=H)
4Ru	M=Ru; (LL) = DPPE; L3 (Z=H; Y=NO$_2$)
4Fe	M=Fe; (LL) = DPPE; L3 (Z=H; Y=NO$_2$)

Scheme 2. Reaction scheme for the synthesis and numbering of the tetrathia-[7]-helicene Ru/Fe derived complexes.

coordinated ligands have been attributed to π-back donation, due to π bonding between the d orbitals of the metal and the π^* orbital of the nitrile group, leading to a decreased C≡N bond order [14,15]. The magnitude of the ν_{CN} negative shift has been clearly related to the electron-donor capacity of the organometallic fragment $[MCp(P–P)]^+$ and the electron-attractor capacity of the substituent group on the chromophore.

^{1}H NMR resonances of the cyclopentadienyl ring are in the characteristic range of monocationic ruthenium(II) and iron(II) complexes. The coordination of TH-[7] derived nitriles leads to a shielding of most of the protons, especially the one in the thiophene ring adjacent to the nitrile group coordinated to the metal. The upfield shift of this proton was more significant for compounds with DPPE as a coligand, up to −1.57 ppm for compound **3Fe**. The unexpected higher shielding (∼0.2 ppm) found for compounds **3Ru** and **3Fe** (with **L2**) than for the analogues **4Ru** and **4Fe** with the better acceptor **L3** might be explained by the spatial effect of the neighbouring uncoordinated C≡N group of **L2**.

^{31}P NMR spectra of the complexes showed a resonance at −144.1 ppm, characteristic of PF_6^-, and resonances of the coordinated phosphines. For compounds **2Ru**, **4Ru** and **4Fe**, the phosphine resonance signals are singlets, but for compounds **1Ru**, **1Fe**, **3Ru** and **3Fe**, the phosphine resonances appear as two doublets with coupling constants ranging from 23.1 to 33.5 Hz, characteristic of phosphorus–phosphorus coupling. This effect may be due to interactions of the phosphines with the opposite end of the helical ligand, causing the unequivalency of the phosphorus atoms. For compounds **4Ru** and **4Fe**, the higher planarity predicted for the helical ligand **L3**, due to the resonant structures originating from the donor (organometallic moiety)-acceptor (NO_2) conjugation, should minimize the referred interactions, while for compound **2Ru**, the less rigid PPh_3 coligands, relatively to DPPE, must allow the phosphorus equivalency.

Table 1
Optical spectral data for the complexes $[M(\eta^5\text{-}C_5H_5)(PP)(L_n)][PF_6]$ and for the free TH[7] derived ligands **L1**, **L2** and **L3**, in CH_2Cl_2 and MeOH (ca. 10^{-4} M) solutions.

Compound	λ_{max}/nm (ε, $M^{-1}\,cm^{-1}$)	
	CH_2Cl_2	MeOH
(L1)	243(27000) 255(sh) 289(16900) 324(13000) 365(sh) 384(13100) 400(13200)	
$[Ru(\eta^5\text{-}C_5H_5)(DPPE)(L1)][PF_6]$ (1Ru)	287(sh) 327(13900) 360(sh) 382(sh) 398(13300) 418(sh)	285(sh) 327(22400) 379(sh) 394(21600) 420(sh)
$[Fe(\eta^5\text{-}C_5H_5)(DPPE)(L1)][PF_6]$ (1Fe)	286(sh) 330(15900) 400(13900) 415(13800) 465(sh)	287(sh) 329(20600) 395(17900) 407(17900) 457(sh)
$[Ru(\eta^5\text{-}C_5H_5)(PPh_3)_2(L1)][PF_6]$ (2Ru)	289(sh) 334(17400) 360(sh) 381(sh) 400(16600) 417(14800)	288(sh) 331(22300) 361(sh) 377(sh) 396(21400) 414(sh)
L2	260(27600) 291(20300) 326(16400) 339(24200) 391(19200) 411(20900)	
$[Ru(\eta^5\text{-}C_5H_5)(DPPE)(L2)][PF_6]$ (3Ru)	290(26300) 325(sh) 339(25300) 391(sh) 409(22300)	288(23500) 301(sh) 323(sh) 338(22300) 390(sh) 407(20600)
$[Fe(\eta^5\text{-}C_5H_5)(DPPE)(L2)][PF_6]$ (3Fe)	291(24300) 341(19000) 398(sh) 414(17500) 471(sh)	326(sh) 340(24900) 396(22700) 412(22900) 460(sh)
L3	254(26000) 276(sh) 349(7000) 430(10700)	
$[Ru(\eta^5\text{-}C_5H_5)(DPPE)(L3)][PF_6]$ (4Ru)	339(sh) 355(19300) 366(sh) 432(20000)	343(sh) 362(17100) 428(16700)
$[Fe(\eta^5\text{-}C_5H_5)(DPPE)(L3)][PF_6]$ (4Fe)	353(11900) 368(sh) 430(16700)	350(sh) 364(15300) 426(19800) 511(sh)

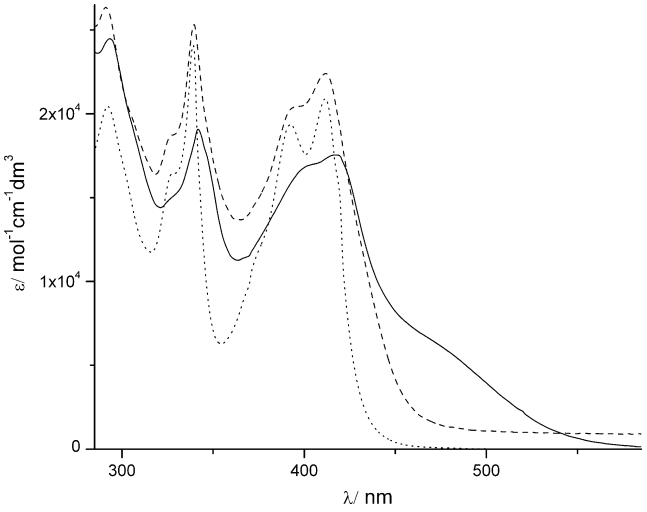

Fig. 1. Electronic spectra of compounds **3Ru**(– – –), **3Fe**(—) and of the ligand **L2**(· · ·) in CH_2Cl_2.

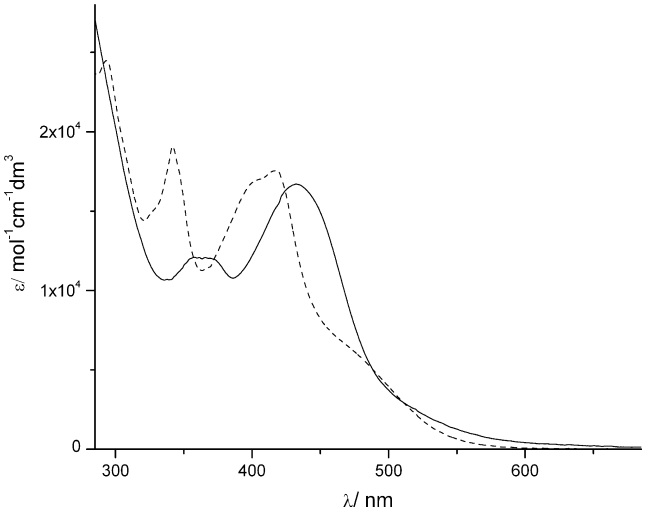

Fig. 2. Electronic spectra of compounds **3Fe**(– – –) and **4Fe**(—) in CH_2Cl_2.

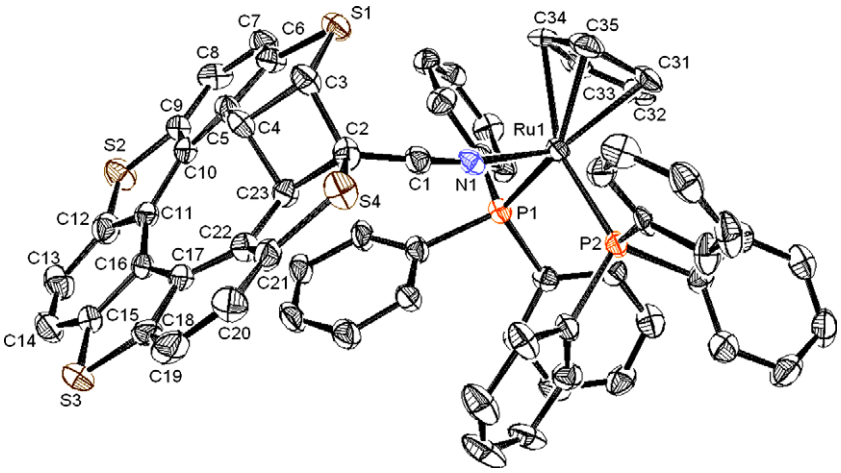

Fig. 3. ORTEP of the cation of compound **2∗Ru**.

2.3. Electronic spectra

Optical absorption spectra of all the complexes $[M(\eta^5\text{-}C_5H_5)(P\text{–}P)(L)][PF_6]$ were recorded in 10^{-4} M dichloromethane and methanol solutions (Table 1), in order to identify the M → L charge transfer and $\pi\text{–}\pi^*$ absorption bands expected for these complexes.

The electronic spectra of the helical ligands show several bands in the UV region due to their extensive π conjugated systems. As would be expected, the introduction of acceptor groups, either CN or NO_2, leads to a bathochromic shift of these bands.

The electronic spectra of the organometallic compounds are characterized by an intense absorption in the range 230–280 nm, attributed to the organometallic fragments $[MCp(P\text{–}P)]^+$, and in the range 280–430 nm, attributed to internal transitions in the TH-[7] derived ligands, by comparison to the free ligand spectra. For compounds **1Fe** and **3Fe**, an additional band is found, as a shoulder, in the ligands lower energy band, attributed to a metal to ligand charge transfer, $d(M^{II}) \rightarrow \pi^*(L)$. For compound **4Fe** no additional band was verified, although enlargement of the lower energy band of the ligand can obscure the existence of any superimposed MLCT band, as was observed before for other compounds with NO_2 substituted nitrile ligands [15e].

In the ruthenium compounds there is no evidence for any MLCT band, although it might be superimposed with the lower energy ligand internal transitions bands. Fig. 1 shows the electronic spectra of compounds $[MCp(DPPE)(NC\{TH\text{-}[7]\}CN)][PF_6]$, **3Ru** and **3Fe**, and of the free ligand **L2**. The existence of a CT band at lower energy is very obvious in compound **3Fe**, in accordance with the spectroscopic data discussed above.

Superimposition of the electronic spectra of compounds **3Fe** and **4Fe**, pictured in Fig. 2, shows that the ~500 nm CT band found in **3Fe** seems also occur in **4Fe**, although in this case it might be obscured by the enlargement of the band at a lower energy.

Table 2
Selected bond distances and bond and torsion angles for compound **2∗Ru**.

Bond distances (Å)			
Ru(1)–N(1)	2.030(5)	P(2)–C(221)	1.850(7)
Ru(1)–Cp[a]	1.8595(6)	P(2)–C(231)	1.829(6)
Ru(1)–P(1)	2.350(2)	N(1)–C(1)	1.147(8)
Ru(1)–P(2)	2.353(2)	C(1)–C(2)	1.433(9)
P(1)–C(111)	1.843(6)	C(2)–C(3)	1.598(9)
P(1)–C(121)	1.831(7)	C(3)–C(4)	1.535(9)
P(1)–C(131)	1.817(7)	C(4)–C(23)	1.519(9)
P(2)–C(211)	1.846(7)	C(23)–C(2)	1.565(9)
Bond angles (°)			
N(1)–Ru(1)–Cp[a]	121.79(14)	C(1)–C(2)–C(3)	115.3(6)
N(1)–Ru(1)–P(1)	87.93(14)	C(2)–C(3)–C(4)	88.8(5)
N(1)–Ru(1)–P(2)	90.83(15)	C(2)–C(23)–C(4)	90.6(5)
P(1)–Ru(1)–P(2)	99.84(6)	C(3)–C(4)–C(23)	91.2(5)
P(1)–Ru(1)–Cp[a]	124.15(5)	C(3)–C(2)–C(23)	87.2(5)
P(2)–Ru(1)–Cp[a]	122.98(5)	C(5)–C(4)–C(23)	106.9(6)
Ru(1)–N(1)–C(1)	169.9(5)	C(4)–C(23)–C(22)	107.7(5)
N(1)–C(1)–C(2)	175.7(7)	C(2)–C(3)–S(1)	119.3(5)
C(1)–C(2)–C(23)	116.4(6)	C(3)–C(2)–S(4)	116.5(5)
Torsion angles (°)			
Ru(1)–N(1)–C(1)–C(2)	29(11)	N(1)-C(1)–C(2)–C(23)	62(9)
N(1)–C(1)–C(2)–C(3)	−38(9)	C(2)–C(3)–C(4)–C(23)	-11.0(5)
N(1)–C(1)–C(2)–S(4)	−175(9)		

[a] Cp ring centroid.

In the ruthenium compounds there is no evidence for any MLCT band, although it might be superimposed with the lower energy ligand internal transitions bands. Fig. 1 shows the electronic spectra of compounds $[MCp(DPPE)(NC\{TH\text{-}[7]\}CN)][PF_6]$, **3Ru** and **3Fe**, and of the free ligand **L2**. The existence of a CT band at lower energy is very obvious in compound **3Fe**, in accordance with the spectroscopic data discussed above.

Superimposition of the electronic spectra of compounds **3Fe** and **4Fe**, pictured in Fig. 2, shows that the ~500 nm CT band found in **3Fe** seems also occur in **4Fe**, although in this case it might be obscured by the enlargement of the band at a lower energy.

2.4. X-ray crystallographic studies

Crystals of compound $[RuCp(PPH_3)_2(NC\{TH\text{-}[7]\})][PF_6] \cdot (CH_3)_2CO$ were obtained by slow diffusion of *n*-hexane in an acetone solution. The results obtained by X-ray diffraction studies showed that the molecular structure of the cation does not correspond to the one expected and confirmed by ^{1}H NMR spectroscopy, due to isomerization of the coordinated ligand **L1**. As can be seen in Fig. 3, the opposite ends of the helical structure of **L1** are bonded (C(2)–C(3) and C(4)–C(23)) in a four-member ring arrangement, with a change in the hybridization of the carbon atoms involved in these bonds from sp^2 to sp^3. A similar phenomenon was reported for another TH[7] derivative [13a], although only one new bond is formed between the helix end rings in that case. Selected bond distances and angles are presented in Table 2. For isomer distinction, the isomer identified by X-ray diffraction is designated as **2∗Ru**.

The referred isomerization was only detected when X-ray diffraction studies were performed, since the initial ^{1}H NMR spectrum of compound **2Ru** is consistent with the predicted structure, with the chemical shifts of the thiophene rings protons and the coupling constant J_{3-4} (5.6 Hz) in the normal ranges for these structures. The isomerization must happen during the slow recrystallization and the **2∗Ru** isomer crystallized preferentially to **2Ru**. The ^{1}H NMR spectrum of **2∗Ru**, described in Section 4, is in accordance with the structure determined by X-ray, showing a significant shielding of protons H(4), H(23) and H(3), compared with **2Ru**, due to the hybridization change in the correspondent carbon atoms. Moreover, H(4) appears as a double doublet, due to coupling with H(3) and H(23), with coupling constants of 6.3 and 8.6 Hz, respectively. The chemical shifts of H(23) and H(3) were attributed based on the coupling constant magnitudes, since J_{23-4} is expected to be higher than J_{3-4} due to the larger H–C–C–H dihedral angle.

Compound **2∗Ru** crystallizes in the centrosymmetric space group $P\bar{1}$. The coordination geometry around the metal centre shows the typical structure of cyclopentadienyl complexes in pseudo-octahedral three-legged piano stool geometry, on the assumption that the cyclopentadienyl ring takes up three coordination sites, with the two PPh_3 phosphorus atoms and the nitrile nitrogen atom occupying the other three sites. The angles P–Ru–P and (C≡)N–Ru–P, close to 90°, and the angles Cp(centroid)–Ru–N(≡C) and Cp(centroide)–Ru–P (121.79(14)–124.15(5)°), along with the distances of the coordinated ligands to the metal centre, are within the range found for η^5-monocyclopentadienylruthenium nitrile derivatives with coordinated phosphines [14,15c,16]. The bond lengths of the cycle formed by atoms C(2), C(3), C(4) and C(23) are in the range 1.519(9)–1.598(9) Å, with bond lengths C(3)–C(4) (1.535(9) Å) and C(2)–C(23) (1.565(9) Å) clearly superior to the analogous ones verified in compounds [MCp(L-L)(NC{BDT}Z)][Y] [14], showing loss of the double bond character. Angles C(5)–C(4)–C(23) (106.9(6) Å) and C(4)–C(23)–C(22) (107.7(5) Å) show the almost superposition of the helix ends.

A possible mechanism to explain the isomerization of **2Ru** to **2∗Ru** is depicted in Scheme 3. It can be assumed that the metal center is involved in the isomerization of the helical ligand. The decoordination of a PPh_3 ligand, followed by the sliding of the nitrile to side-on (four-electron-donor) coordination allow the interaction of the metal centre with H(3). Nucleophilic attack at C(3)

Table 3
Interplanar angles, θ, between adjacent rings and the terminal rings of the thiophene rings (°) and the mean-square atom deviations, Δ, from ring least-squares planes, for compound **2∗Ru**.

θ		Δ	
Ring(1)–ring(2)	6.33	ring(1)	0.0063
Ring(2)–ring(3)	6.64	ring(2)	0.0590
Ring(3)–ring(4)	4.57	ring(3)	0.0250
Ring(4)–ring(5)	4.86	ring(4)	0.0279
Ring(5)–ring(6)	8.01	ring(5)	0.0295
Ring(6)–ring(7)	6.80	ring(6)	0.0489
Ring(1)–ring(7)	4.43	ring(7)	0.0235

Ring(1): (C(3), C(4), C(5), C(6), S(1)); ring(2): (C(5), C(6), C(7), C(8), C(9), C(10)); ring(3): (C(9), C(10), C(11), S(2)); ring(4): (C(11), C(12), C(13), C(14), C(15), C(16)); ring(5): (C(15), C(16), C(17), C(18), S(3)); ring(6): (C(17), C(18), C(19), C(20), C(21), C(22)); ring(7): (C(21), C(22), C(23), C(24), S(4)).

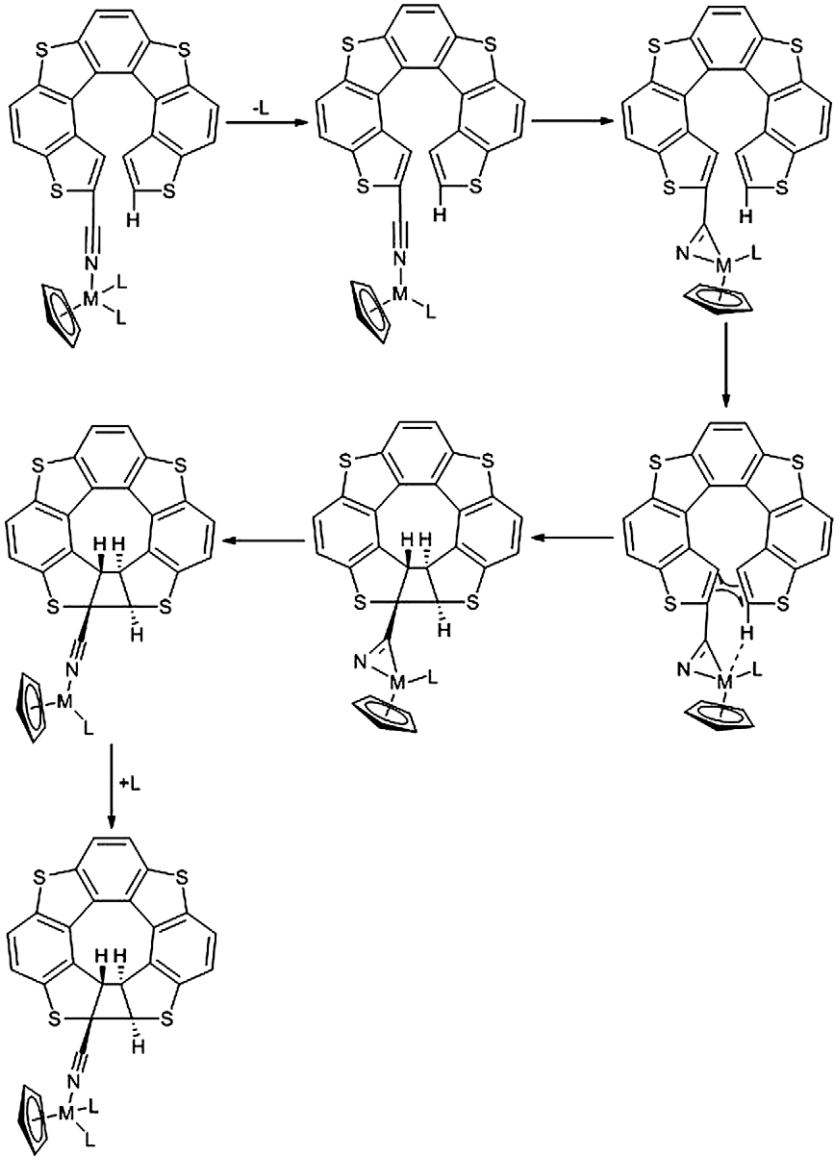

Scheme 3. Proposed mechanism for formation of **2∗Ru**.

Table 4
Intermolecular contacts for compound **2∗Ru**.

2∗Ru	
C(35)–H(35)···F(1)	2.568
C(124)–H(124)···F(4)	2.647
C(3)–H(3)···F(4)	2.619
C(13)–H(13)···O(100)	2.491

and subsequent rearrangement results in bonding between the helix ends. Return of the nitrile to end-on coordination and coordination of PPh_3 affords **2∗Ru**. This mechanism is supported by the fact that isomerization was only detected in one complex, and not in the free ligand, and this being the complex with coordinated monodentate phosphines.

The dihedral angles between adjacent rings and terminal rings of the helicene ligand of compound **2∗Ru,** as well as the mean-square atom deviations Δ from the ring least-squares planes, are listed in Table 3. The planarity of the aromatic rings in the molecules is apparent from the mean deviations of the atoms from the least-squares plane of the ring (Table 3). The terminal rings 1 and 7 have an almost flat configuration, but the planarity is poorer towards the middle thiophene rings and is poorest in the benzene rings. Also, a decrease of the dihedral angle towards the middle part of the helix can be noticed, although the deformation of the rings from planarity does not follow the same correlation. This behavior is opposite to that observed in free TH[7] [17]. A possible explanation for this different structural arrangement is the isomerization of the helical ligand that forces a smaller aperture in the two terminal thiophene rings, as reflected by the dihedral angle between the rings 1 and 7 (4.43° vs. 45.9° for free TH[7]).

The pitch of the helix in **2∗Ru** compound is very similar to the free TH[7] ligand (14.30 Å vs. 14.03 Å), since the two thiahelicenes have the same number of rings [18].

The evaluation of the crystal packing of **2∗Ru** revealed the formation of pseudo dimeric units, with parallel alignment of the chromophores of distinct cations, via intermolecular interactions with the PF_6 anion and one acetone molecule (Table 4), reinforced through π–π interactions of the helical ligand.

This pseudo dimeric arrangement is illustrated in Fig. 4, where it can also be seen that these units are constituted by two enantiomers, (+) and (−), relative to the helix orientation.

Analysis of the crystal packing disclosed an interesting supramolecular array for this compound, which displays holes in the *c* direction, as illustrated in Fig. 5, suggesting that this network can possibly be used for selectively storing guests material [19]. These holes, that have an almost square shape, have the smaller dimensions between two fluorine atoms of the counter-ion PF_6, 4.851 Å, and two of the carbons of the acetone solvent molecule, 4.750 Å. The holes are created by two of the parallel lines produced via intermolecular interactions involving the helicene–PF_6–acetone. A similar array with a significant degree of porosity was verified for the compound $[RuCp(PPh_3)_2(NC(BDT))][PF_6]$ (BDT = benzo[1,2-b;4,3-b′]dithiophene) [14], although the holes aperture is larger in this compound.

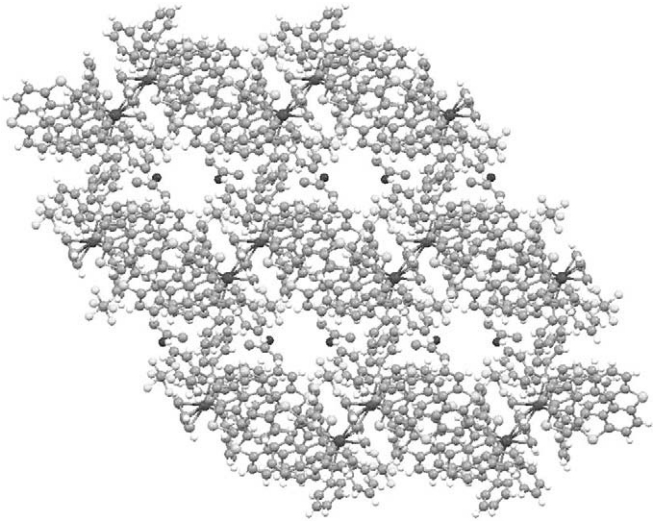

Fig. 5. Supramolecular arrangement of the compound **2∗Ru**, displaying holes along direction *c*.

3. Conclusion

We have described here the synthesis of the new organometallic complexes $[MCp(P–P)(NC\{TH\text{-}[7]\text{-}Y\}Z)][PF_6]$ (M = Ru, Fe, P–P = DPPE, Y = H, NO_2, Z = H, C≡N; M = Ru, L-L = $2PPh_3$, Y = H, Z = H), with coordinated helical ligands derived from tetrathia-[7]-helicene. Spectroscopic data revealed the electron-donor effect of the organometallic fragments $[MCp(P–P)]^+$. The magnitude of this effect depends on the metal and on the presence and/or position of the acceptor group (C≡N, NO_2), showing a good conjugation between the metal centre and the acceptor group on the chromophore.

The three new substituted tetrathia-[7]-helicene derivatives, synthesized in this work and used as ligands in the presented organometallic complexes, may also be interesting as organic materials for NLO purposes, according to the significant β values predicted by theoretical studies for other tetrathia-[7]-helicene derivatives [20].

The major interest in this family of compounds is the intrinsic chirality for NLO purposes, which has not yet been exploited, since the TH[7] ligands were prepared as a racemic mixture. Nevertheless, the synthetic procedure developed in the present work is valid for the synthesis of the pure isomers complexes, starting from the respective isomerically pure TH[7], bearing in mind that isomer inter-conversion is not possible.

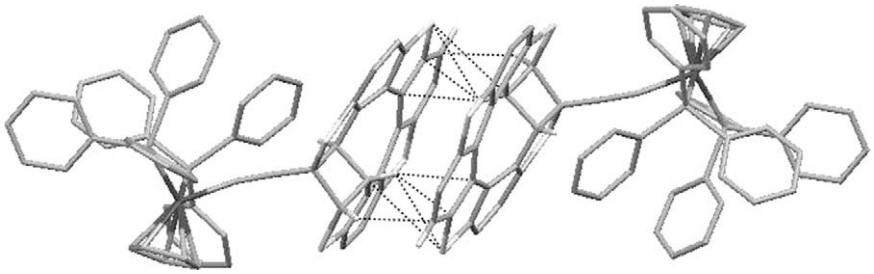

Fig. 4. Dimeric units of compound **2∗Ru**, showing intermolecular π–π interactions of the helical ligand.

4. Experimental

4.1. General procedures

All experiments were carried out under nitrogen atmosphere using standard Schlenk techniques. All of the solvents used were dried using standard methods [21]. The starting materials were prepared following the methods described in the literature: [Ru(η^5-C_5H_5)(DPPE)Cl] and [Ru(η^5-C_5H_5)(PPh_3)$_2$Cl] [22]; [Fe(η^5-C_5H_5)(DPPE)I] [15c]; tetrathia-[7]-helicene and tetrathia-[7]-helicene-2-carbox aldehyde [16a]. FT-IR spectra were recorded in a Mattson Satelite FTIR spectrophotometer with KBr; only significant bands are quoted in the text. ^{1}H and ^{31}P NMR spectra were recorded on a Brüker Avance 400 spectrometer at the probe temperature. ^{1}H (DMSO-d_6) chemical shifts are reported in parts per million (ppm) downfield from internal Me_4Si and coupling constants are reported in Hertz; ^{31}P (DMSO-d_6) NMR spectra are reported in ppm downfield from the external standard, 85% H_3PO_4. Elemental analyses were obtained at the Laboratório de Análises, Instituto Superior Técnico, using a Fisons Instruments EA1108 system. Data acquisition, integration and handling were performed using a PC with software package EAGER-200 (Carlo Erba Instruments). Electronic spectra were recorded at room temperature on a Jasco V-560 spectrometer in the range 200–900 nm.

4.2. Synthesis of the organic ligands

4.2.1. Tetrathia-[7]-helicene-2-carbonitrile (**L1**)

An $H_2NOH \cdot HCl$ (0.14 g, 2 mmol) solution in pyridine (4 mL) was added to a stirred solution of tetrathia-[7]-helicene-2-carbaldehyde (0.22 g, 0.5 mmol) in pyridine (5 mL), cooled to 5 °C. After stirring for 1 h at 5 °C, acetic anhydride (1 mL) was added, and the mixture was refluxed for 2 h. After cooling, the mixture was poured onto ice and the resulting precipitate was dissolved in CH_2Cl_2 (30 mL), washed with a saturated solution of $NaHCO_3$ and water, and dried over $MgSO_4$. The solvent was removed under reduced pressure and the product was purified by flash column chromatography (eluent:*n*-hexane/CH_2Cl_2 1:1), affording 0.10 g (47%) of pure tetrathia-[7]-helicene-2-carbonitrile as a yellow solid. *Anal.* (%) Calc. for $C_{23}H_9NS_4 \cdot 0.1C_6H_{14}$: C, 64.99; H, 2.40; N, 3.21. Found: C, 65.72; H, 2.13; N, 3.23. IR (KBr, cm^{-1}): ν(CN) 2206. ^{1}H NMR (DMSO-d_6): 6.49 (d, 1H, J_{HH} = 5.6), 7.23 (s, 1H) 7.40 (d, 1H, J_{HH} = 5.6), 8.28 (d, 1H, J_{HH} = 8.4), 8.29 (m, 4H), 8.51 (d, 1H, 8.8).

4.2.2. Tetrathia-[7]-helicene-2,13-dicarbonitrile (**L2**)

A *n*-BuLi 2.0 M pentane solution (0.55 mL, 1.1 mmol) was added dropwise to a stirred solution of tetrathia-[7]-helicene (0.20 g, 0.5 mmol) in dry THF (20 mL) at −78 °C. The solution was stirred for 40 min at −78 °C, and the resulting dark orange solution was treated with dry DMF (0.11 mL, 1.2 mmol). After 4 h at −78 °C, the solution was warmed up to room temperature and quenched with a saturated aqueous solution of NH_4Cl (5 mL). The THF was removed under reduced pressure, and the crude was taken up with CH_2Cl_2 (20 mL) and washed with water and a saturated solution of NH_4Cl. The solvent was removed under reduced pressure, affording tetrathia-[7]-heliceno-2,2′-dicarbaldehyde, as a dark oil, used without further purification. The product was dissolved in pyridine, cooled to 5 °C, and an $H_2NOH \cdot HCl$ (0.14 g, 2.0 mmol) solution in pyridine (4 mL) was added. After stirring for 5 min at 5 °C, acetic anhydride (1 mL) was added and the mixture was refluxed for 2 h. After cooling, the mixture was poured onto ice and the resulting precipitate was dissolved in CH_2Cl_2 (20 mL), washed with water and dried over $MgSO_4$. The product was purified by flash column chromatography (eluent:*n*-hexane/CH_2Cl_2 2:3), affording 0.05 g (25%) of pure tetrathia-[7]-helicene-2,13-dicarbonitrile as a yellow solid. *Anal.* (%) Calc. for $C_{24}H_8N_2S_4$: C, 63.69; H, 1.78; N, 6.19. Found: C, 64.02; H, 1.86; N, 5.99. IR (KBr, cm^{-1}): ν(CN) 2209. ^{1}H NMR (DMSO-d_6): 7.21 (s, 2H), 8.46 (s, 2H), 8.49 (d, 2H, J_{HH} = 8.8), 8.58 (d, 2H, J_{HH} = 8.8).

4.2.3. Tetrathia-[7]-helicene-?-nitro-2-carbonitrile (**L3**)

Nitric acid (0.02 mL, 0.35 mmol) was added to a stirred solution of tetrathia-[7]-helicene-2-carbonitrile (0.11 g, 0.26 mmol) in acetic anhydride (8 mL), cooled to 5 °C. After 1 h, the solution was poured onto ice and the resultant precipitate was dissolved in CH_2Cl_2 (15 mL). The solution was washed with a saturated solution of $NaHCO_3$, water, dried over $MgSO_4$ and the solvent removed under reduced pressure. The product was purified by flash column chromatography (eluent:*n*-hexane/CH_2Cl_2 2:3), affording 0.05 g (41%) of tetrathia-[7]-helicene-?-nitro-2-carbonitrile as an orange solid. IR (KBr, cm^{-1}): ν(CN) 2215, ν(NO_2) 1507 and 1316, δ (NO_2) 731. ^{1}H NMR (DMSO-d_6): 6.65 (d, 1H, J_{HH} = 5.6), 7.29 (s, 1H), 7.57 (d, 1H, J_{HH} = 5.6), 8.45 (d, 1H, J_{HH} = 8.8), 8.54 (m, 3H), 9.60 (s, 1H).

4.3. Synthesis of the complexes [M(η^5-C_5H_5)(P–P)(NC{TH-[7]-Y}Z)][PF_6]

Complexes of the general formula [M(η^5-C_5H_5)(P–P)(NC{TH-[7]-Y}Z)][PF_6] were prepared by halide abstraction from the parent neutral complexes [M(η^5-C_5H_5)(LL)X] (1 mmol) with $TlPF_6$ (1 mmol) in dichloromethane, in the presence of a slight excess (1.1 mmol) of the ligands tetrathia-[7]-helicene-2-carbonitrile (**L1**), tetrathia-[7]-helicene-2,2′-carbonitrile (**L2**) or tetrathia-[7]-helicene-?-nitro-2-carbonitrile (**L3**), at reflux for 48 h under an inert atmosphere. After cooling to room temperature, filtering and removing the solvent, the complexes were washed with *n*-hexane (3 × 15 mL) and recrystallized from dichloromethane/*n*-hexane or acetone/*n*-hexane, giving crystalline products.

4.3.1. [Ru(η^5-C_5H_5)(DPPE)(NC{TH-[7]})][PF_6] (**1Ru**)

Orange. Yield: 48%. Recrystallized from dichloromethane/*n*-hexane. *Anal.* (%) Calc. for: $C_{54}H_{38}NS_4P_3F_6Ru$: C, 57.04; H, 3.37; N, 1.23. Found: C, 57.30; H, 3.56; N, 1.60. IR (KBr, cm^{-1}): ν(C–H, η^5-C_5H_5) 3051, ν(CN) 2210, ν(PF_6^-) 839; ^{1}H NMR ($(CD_3)_2SO$): 2.65 (m, 4H, –CH_2–), 4.91 (s, 5H, η^5-C_5H_5), 6.06 (s, 1H), 6.22 (d, 1H, J_{HH} = 5.6), 7.04 (d, 1H, J_{HH} = 5.6), 7.24 (m, 4H, C_6H_5, DPPE), 7.36 (m, 6H, C_6H_5, DPPE), 7.51 (m, 6H, C_6H_5, DPPE), 7.78 (m, 4H, C_6H_5, DPPE), 8.28 (d, 1H, J_{HH} = 8.8), 8.41 (d, 1H, J_{HH} = 8.4), 8.47 (m, 4H). ^{31}P NMR ($(CD_3)_2SO$): −144.1 (qt, PF_6^-, J_{PF} = 711.0), 78.3 (d, DPPE, J_{PP} = 24.5), 79.5 (d, DPPE, J_{PP} = 24.5).

4.3.2. [Fe(η^5-C_5H_5)(DPPE)(NC{TH-[7]})][PF_6] (**1Fe**)

Red. Yield: 46%. Recrystallized from dichloromethane/*n*-hexane. *Anal.* (%) Calc. for $C_{54}H_{38}NS_4P_3F_6Fe \cdot 0.3CH_2Cl_2$: C, 58.54; H, 3.48; N, 1.25. Found: C, 58.29; H, 3.78; N, 1.26. IR (KBr, cm^{-1}): ν(C–H, η^5-C_5H_5) 3052, ν(CN) 2193, ν(PF_6^-) 840. ^{1}H NMR ($(CD_3)_2SO$): 2.46 (m, 2H, –CH_2–), 2.62 (m, 2H, –CH_2–), 4.53 (s, 5H, η^5-C_5H_5), 5.97 (s, 1H), 6.22 (d, 1H, J_{HH} = 5.6), 7.04 (d, 1H, J_{HH} = 5.6), 7.06 (m, 4H, C_6H_5, DPPE), 7.56 (m, 12H, C_6H_5, DPPE), 7.81 (m, 4H, C_6H_5, DPPE), 8.25 (d, 1H, J_{HH} = 8.8), 8.43 (m, 5H). ^{31}P NMR ($(CD_3)_2SO$): −144.1 (qt, PF_6^-, J_{PF} = 710.2), 96.4 (d, DPPE, J_{PP} = 33.2), 96.8 (d, DPPE, J_{PP} = 33.5).

4.3.3. [Ru(η^5-C_5H_5)(PPh_3)$_2$(NC{TH-[7]})][PF_6] (**2Ru**)

Orange. Yield: 27%. Recrystallized from acetone/*n*-hexane. IR (KBr, cm^{-1}): ν(C–H, η^5-C_5H_5) 3053, ν(CN) 2210, ν(PF_6^-) 840. ^{1}H NMR ($(CD_3)_2SO$): 4.61 (s, 5H, η^5-C_5H_5), 6.45 (d, 1H, J_{HH} = 5.6), 6.90 (s, 1H), 7.21 (m, 12H, C_6H_5, PPh_3), 7.31 (m, 12H, C_6H_5, PPh_3), 7.40 (d, 1H, J_{HH} = 5.6), 7.44 (m, 6H, C_6H_5, PPh_3), 8.14 (d, 1H, J_{HH} = 8.8), 8.24 (d, 1H, J_{HH} = 8.8), 8.40 (d, 1H, J_{HH} = 8.8), 8.43 (d,

1H, J_{HH} = 8.4), 8.47 (d, 1H, J_{HH} = 8.4), 8.55 (d, 1H, J_{HH} = 8.8). ^{31}P NMR ($(CD_3)_2SO$): −144.1 (qt, PF_6^-, J_{PF} = 711.1), 41.31 (s, PPh_3).

(***2*Ru***): Orange. ^{1}H NMR ($(CD_3)_2SO$): 3.29 (d, 1H, H(3), J_{3-4} = 6.4), 4.41 (dd, 1H, H(4), J_{4-3} = 6.3, J_{4-23} = 8.6), 5.27 (d, 1H, H(23), J_{23-4} = 8.8), 6.76 (m, 5H, C_6H_5, PPh_3), 6.96 (m, 6H, C_6H_5, PPh_3), 7.07 (m, 6H, C_6H_5, PPh_3), 7.17 (m, 5H, C_6H_5, PPh_3), 7.26 (m, 3H, C_6H_5, PPh_3), 7.35 (m, 3H, C_6H_5, PPh_3), 7.48 (m, 2H, C_6H_5, PPh_3), 7.62 (d, 1H, J_{HH} = 8.3), 7.69 (d, 1H, J_{HH} = 8.4), 7.99 (d, 1H, J_{HH} = 8.3), 8.07 (d, 1H, J_{HH} = 8.3), 8.39 (d, 1H, J_{HH} = 8.6), 8.42 (d, 1H, J_{HH} = 8.4).

4.3.4. [Ru(η^5-C_5H_5)(DPPE)(NC{TH-[7]}CN)][PF_6] (***3Ru***)

Dark red. Yield: 56%. Recrystallized from dichloromethane/*n*-hexane. *Anal.* (%) Calc. for $C_{55}H_{37}N_2S_4P_3F_6Ru$: C, 56.84; H, 3.21; N, 2.41. Found: C, 56.40; H, 3.38; N, 2.41. IR (KBr, cm^{-1}): ν(C–H, η^5-C_5H_5) 3051, ν(CN) 2212, $\nu(PF_6^-)$ 839. ^{1}H NMR ($(CD_3)_2SO$): 2.20 (m, 2H, –CH_2–), 2.79 (m, 2H, –CH_2–), 4.89 (s, 5H, η^5-C_5H_5), 5.70 (s, 1H), 6.88 (s, 1H), 7.22 (m, 4H, C_6H_5, DPPE), 7.50 (m, 12H, C_6H_5, DPPE), 7.91 (m, 4H, C_6H_5, DPPE), 8.37 (d, 2H, J_{HH} = 8.8), 8.51 (m, 4H), 8.71 (d, 2H, H_6, J_{HH} = 8.8). ^{31}P NMR ($(CD_3)_2SO$): −144.1 (qt, PF_6^-, J_{PF} = 711.4), 78.3 (d, DPPE, J_{PP} = 25.1), 79.7 (d, DPPE, J_{PP} = 23.1).

4.3.5. [Fe(η^5-C_5H_5)(DPPE)(NC{TH-[7]}CN)][PF_6] (***3Fe***)

Dark red. Yield: 59%. Recrystallized from dichloromethane/*n*-hexane. *Anal.* (%) Calc. for $C_{55}H_{37}N_2S_4P_3F_6Fe$: C, 59.15; H, 3.34; N, 2.51. Found: C, 59.01; H, 3.70; N, 2.14. IR (KBr, cm^{-1}): ν(C–H, η^5-C_5H_5) 3052, ν(CN) 2191, $\nu(PF_6^-)$ 839. ^{1}H NMR ($(CD_3)_2SO$): 2.37 (m, 2H, –CH_2–), 2.70 (m, 2H, –CH_2–), 4.52 (s, 5H, η^5-C_5H_5), 5.64 (s, 1H), 6.85 (s, 1H), 7.26 (m, 4H, C_6H_5, DPPE), 7.56 (m, 12H, C_6H_5, DPPE), 7.93 (m, 4H, C_6H_5, DPPE), 8.35 (d, 2H, J_{HH} = 8.8), 8.67 (d, 2H, H_6, J_{HH} = 8.8). ^{31}P NMR ($(CD_3)_2SO$): −144.1 (qt, PF_6^-, J_{PF} = 710.6), 96.8 (d, DPPE, J_{PP} = 33.4), 97.4 (d, DPPE, J_{PP} = 32.7).

4.3.6. [Ru(η^5-C_5H_5)(DPPE)(NC{TH-[7]-NO_2})][PF_6] (***4Ru***)

Dark red. Yield 40%. Recrystallized from dichloromethane/*n*-hexane. *Anal.* (%) Calc. for $C_{54}H_{37}N_2O_2S_4P_3F_6Ru$: C, 54.87; H, 3.15; N, 2.37. Found: C, 54.52; H, 3.56; N, 2.63. IR (KBr, cm^{-1}): ν(C–H, η^5-C_5H_5) 3054, ν(CN) 2214, $\nu(NO_2)$ 1507 and 1314, $\delta(NO_2)$ 730, $\nu(PF_6^-)$ 839. ^{1}H NMR ($(CD_3)_2SO$): 2.34 (m, 2H, –CH_2–), 2.67 (m, 2H, –CH_2–), 4.84 (s, 5H, η^5-C_5H_5), 5.98 (s, 1H), 6.40 (d, 1H, J_{HH} = 5.6), 7.29 (d, 1H, J_{HH} = 5.6), 7.35 (m, 6H, C_6H_5, DPPE), 7.51 (m, 6H, C_6H_5, DPPE), 7.72 (m, 8H, C_6H_5, DPPE), 8.33 (d, 1H, J_{HH} = 8.8), 8.52 (d, 1H, J_{HH} = 8.8), 8.59 (s, 2H), 9.75 (s, 1H). ^{31}P NMR ($(CD_3)_2SO$): −144.1 (qt, PF_6^-, J_{PF} = 712.7), 78.7 (s, DPPE).

4.3.7. [Fe(η^5-C_5H_5)(DPPE)(NC{TH-[7]-NO_2})][PF_6] (***4Fe***)

Dark red. Yield 44%. Recrystallized from dichloromethane/*n*-hexane. *Anal.* (%) Calc. for $C_{54}H_{37}N_2O_2S_4P_3F_6Fe \cdot 0.3CH_2Cl_2$: C, 56.11; H, 3.26; N, 2.41. Found: C, 55.91; H, 3.39; N, 3.08. IR (KBr, cm^{-1}): ν(C–H, η^5-C_5H_5) 3052, ν(CN) 2191, $\nu(NO_2)$ 1507 and 1313, $\nu(PF_6^-)$ 839. ^{1}H NMR ($(CD_3)_2SO$): 2.12 (m, 2H, –CH_2–), 2.35 (m, 2H, –CH_2–), 4.57 (s, 5H, η^5-C_5H_5), 5.90 (s, 1H), 6.39 (d, 1H, J_{HH} = 5.6), 7.32 (d, 1H, J_{HH} = 5.6), 7.35 (m, 8H, C_6H_5, DPPE), 7.55 (m, 8H, C_6H_5, DPPE), 7.74 (m, 4H, C_6H_5, DPPE), 8.30 (d, 1H, J_{HH} = 8.8), 8.49 (d, 1H, J_{HH} = 8.8), 8.57 (s, 2H), 9.72 (s, 1H). ^{31}P NMR ($(CD_3)_2SO$): −144.1 (qt, PF_6^-, J_{PF} = 710.2), 97.0 (s, DPPE).

4.4. X-ray crystallography

X-ray data for compound **2*Ru** was collected on a Bruker AXS APEX CCD area detector diffractometer at 293(2) K using graphite-monochromated Mo Kα (λ = 0.71073 Å) radiation. Intensity data were corrected for Lorentz polarization effects. Empirical absorption corrections, using SADABS [23], were applied and the data reduction was done with SMART and SAINT programs [24]. All structures were solved by direct methods with SIR97 [25] and refined by full-matrix least-squares on F^2 with SHELXL97 [26], both included in the package of programs WINGX-Version 1.70.01 [27].[7] Non-hydrogen atoms were refined with anisotropic thermal parameters, whereas H-atoms were placed in idealised positions and allowed to refine riding on the parent C atom. Graphical representations were prepared using ORTEP [28] and Mercury 1.1.2 [29]. Crystallographic data: crystal colour orange, crystal habit plate, crystal dimensions 0.10 × 0.09 × 0.02 mm, empirical formula $C_{67}H_{44}F_6NO_3P_3S_3Ru$, M = 1315.25, crystal system triclinic, space group $\bar{P}$, a = 14.038(3), b = 14.992(3), c = 16.937(3) Å, α = 110.185(7), β = 103.719(6), γ = 102.132(6)°, V = 3079.0(10) Å^3, Z = 2, $D_{calc.}$ = 1.765 g cm^{-3}, T = 150(2) K, reflections collected/unique 23 172/13 568, parameters 748, final R indices [$I > 2\sigma(I)$]: R_1 = 0.0687; wR_2 = 0.1422.

Supplementary data

CCDC 688367 contains the supplementary crystallographic data for **2*Ru**. These data can be obtained free of charge via http://www.ccdc.cam.ac.uk/conts/retrieving.html, or from the Cambridge Crystallographic Data Centre, 12 Union Road, Cambridge CB2 1EZ, UK; fax: (+44) 1223-336-033; or e-mail: deposit@ccdc.cam.ac.uk.

Acknowledgements

The authors thank Fundação Para a Ciência e Tecnologia (FCT) for financial support of Project POCTI/QUI/48443/2002. Pedro Florindo thanks FCT for his Ph.D. Grant (SFRH/BD/12432/2003).

E. Licandro and S. Maiorana acknowledge joint financial support from the Ministero dell'Istruzione, dell'Università e della Ricerca Scientifica (MUR), Rome, and the University of Milan (FIRB project, Bando 2003, Progetto RBNE033KMA, title of the project: "Molecular compounds and hybrid nanostructured materials with resonant and non resonant optical properties for photonic devices" and the University of Milan for the PRIN 2005 project: "Nuovi sistemi catalitici stereoselettivi e sintesi stereoselettiva di molecole funzionali". Centro di Eccellenza CIMAINA and the C.N.R. of Rome is also acknowledged.

References

[1] H.S. Nalwa, Appl. Organomet. Chem. 5 (1991) 349.
[2] N.J. Long, Angew. Chem., Int. Ed. Engl. 34 (1995) 21.
[3] S.R. Marder, in: D.W. Bruce, D. O'Hare (Eds.), Inorganic Materials, 2nd ed., Wiley, Chichester, 1996, p. 121.
[4] I.R. Whittall, A.M. McDonagh, M.G. Humphrey, M. Samoc, Adv. Organomet. Chem. 42 (1998) 291.
[5] E. Goovaerts, W.E. Wenseleers, M.H. Garcia, G.H. Cross,in: H.S. Nalwa (Ed.), Handbook of Advanced Electronic and Photonic Materials, vol. 9, 2001, p. 127 (Chapter 3).
[6] S. Di Bella, Chem. Soc. Rev. 30 (2001) 355.
[7] M. Kauranen, T. Verbiest, A. Persoons, J. Nonlinear Opt. Phys. Mater. 8 (1999) 171.
[8] T. Petralli-Mallow, T.M. Wong, J.D. Byers, H.I. Yee, J.M. Hicks, J. Phys. Chem. 97 (1993) 1383.
[9] M. Kauranen, T. Verbiest, E.W. Meijer, E.E. Havinga, M.N. Teerenstra, A.J. Schouten, R.J.M. Nolte, A. Persoons, Adv. Mater. (Weinheim, Germany) 7 (1995) 641.
[10] R.H. Martin, Angew. Chem., Int. Ed. 13 (1974) 649.
[11] (a) T. Verbiest, S. Vanelshocht, M. Kauranen, L. Hellemans, J. Snauwaert, C. Nuckolls, T.J. Katz, A. Persoons, Science 282 (1998) 913;
(b) S. Sioncke, S. Van Elshocht, T. Verbiest, A. Persoons, M. Kauranen, K.E.S. Phillips, T.J. Katz, J. Chem. Phys. 113 (2000) 7578;
(c) D. Belijonne, Z. Shuai, J.L. Brédas, M. Kauranen, T. Verbiest, A. Persoons, J. Chem. Phys. 104 (1998) 1301;
(d) L. Minuti, A. Taticchi, A. Marrocchi, E. Gacs-Baitz, R. Galeazzi, Eur. J. Org. Chem. (1999) 3155;
(e) H. Soon Choi, K.S. Kim, J. Phys. Chem. B 104 (2000) 11006.
[12] H. Ashitaka, H. Sasabe, Non-linear Opt. 14 (1995) 81.
[13] (a) S. Maiorana, A. Papagni, E. Licandro, R. Annunziata, P. Paravidino, D. Perdicchia, C. Giannini, K. Clays, A. Persoons, Tetrahedron 59 (2003) 6481;
(b) C. Baldoli, A. Bossi, C. Giannini, E. Licandro, S. Maiorana, D. Perdichia, Synlett (2005) 1137;

(c) A. Bossi, S. Maiorana, C. Graiff, A. Tiripicchio, E. Licandro, Eur. J. Org. Chem. 27 (2007) 4499;
(d) C. Baldoli, C. Giannini, E. Licandro, S. Maiorana, M. Monteforte, C. Rigamonti, M.T. Ticozzelli, Synthesis 21 (2006) 3670;
(e) T. Kawasaki, K. Suzuki, E. Licandro, A. Bossi, S. Maiorana, K. Soai, Tetrahedron: Asymmetry 17 (14) (2006) 2050.
[14] M.H. Garcia, P. Florindo, M.F.M. Piedade, M.T. Duarte, M.P. Robalo, J. Heck, C. Wittenburg, J. Holtmann, E. Licandro, J. Organomet. Chem., doi: 10.1016/j.jorganchem.2008.05.035.
[15] (a) A.R. Dias, M.H. Garcia, M.P. Robalo, M.L.H. Green, K.K. Lai, A.J. Pulham, S.M. Klueber, G. Balavoine, J. Organomet. Chem. 453 (1993) 241;
(b) A.R. Dias, M.H. Garcia, J.C. Rodrigues, M.L.H. Green, S.M. Kuebler, J. Organomet. Chem. 475 (1994) 241;
(c) M.H. Garcia, M.P. Robalo, A.R. Dias, M.F.M. Piedade, A. Galvão, M.T. Duarte, W. Wenseleers, E. Goovaerts, J. Organomet. Chem. 619 (2001) 252;
(d) W. Wenseleers, A.W. Gerbrandij, E. Goovaerts, M.H. Garcia, M. Paula Robalo, Paulo J. Mendes, João C. Rodrigues, A.R. Dias, J. Mater. Chem. 8 (1998) 925;
(e) M.H. Garcia, P.J. Mendes, M.P. Robalo, A.R. Dias, J. Campo, W. Wenseleers, E. Goovaerts, J. Organomet. Chem. 692 (2007) 3027.
[16] (a) R.L. Cordiner, D. Albesa-Jové, R.L. Roberts, J.D. Farmer, H. Puschmann, D. Corcoran, A.E. Goeta, J.A.K. Howard, P.J. Low, J. Organomet. Chem. 690 (2005) 4908;
(b) R.L. Cordiner, D. Corcoran, D.S. Yufit, A.E. Goeta, J.A.K. Howard, P.J. Low, J. Chem. Soc., Dalton Trans. (2003) 3541.
[17] H. Nakagawa, A. Obata, K. Yamada, H. Kawazura, M. Konno, H. Miyamae, J. Chem. Soc., Perkin Trans. II (II) (1985) 1899.
[18] T. Caronna, M. Catellani, S. Luzzati, L. Malpezzi, S.V. Meille, A. Mele, C. Richter, R. Sinfisi, Chem. Mater. 13 (2001) 3906.
[19] (a) K.E. Maly, E. Gagnon, T. Maris, J.D. Wuest, J. Am. Chem. Soc. 129 (2007) 4306;
(b) X. Lin, J. Jia, X. Zhao, K.M. Thomas, A.J. Blake, G.S. Walker, N.R. Champness, P. Hubberstey, M. Schröder, Angew. Chem., Int. Ed. 45 (2006) 7358.
[20] (a) C.A. Daul, I. Ciofini, V. Weber, Int. J. Quantum Chem. 91 (2003) 297;
(b) A. Bossi, E. Licandro, S. Maiorana, C. Rigamonti, S. Righetto, G.R. Stephenson, M. Spassova, E. Botek, B. Champagne, J. Phys. Chem. ACS ASAP (2008);
(c) B. Campagne, J.-M. André, E. Botek, E. Licandro, S. Maiorana, A. Bossi, K. Clays, A. Persoons, ChemPhysChem 5 (2004) 1438.
[21] D.D. Perrin, W.L.F. Amarego, D.R. Perrin, Purification of Laboratory Chemicals, 2nd ed., Pergamon, New York, 1980.
[22] G.S. Ashby, M.I. Bruce, I.B. Tomkins, R.C. Walli, Aust. J. Chem. 32 (1979) 1003.
[23] SADABS: Area-Detector Absorption Correction, Bruker AXS Inc., Madison, WI, 2004.
[24] SAINT: Area-Detector Integration Software, Version 7.23, Bruker AXS Inc., Madison, WI, 2004.
[25] A. Altomare, M.C. Burla, M. Camalli, G. Cascarano, G. Giacovazzo, A. Guagliardi, A.G.G. Moliterini, G. Polidoro, R. Spagna, J. Appl. Crystallogr. 32 (1999) 115.
[26] G.M. Sheldrick, SHELXL-97: Program for the Refinement of Crystal Structure, University of Gottingen, Germany, 1997.
[27] L.J. Farrugia, J. Appl. Crystallogr. 32 (1999) 837.
[28] L.J. Farrugia, J. Appl. Crystallogr. 30 (1997) 565.
[29] C.F. Macrae, P.R. Edgington, P. McCabe, E. Pidcock, G.P. Shields, R. Taylor, M. Towler, J. Van de Streek, J. Appl. Crystallogr. 39 (2006) 453.